Applied Energy 353 (2024) 122045

Contents lists available at ScienceDirect

Applied Energy

journal homepage: www.elsevier.com/locate/apenergy

Exhaust gas aftertreatment to minimize NO_X emissions from hydrogen-fueled internal combustion engines

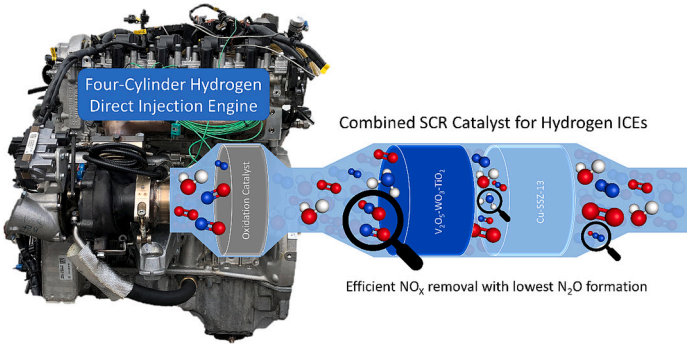
Can Özyalcin [a], Stefan Sterlepper [a,*], Sebastian Roiser [b], Helmut Eichlseder [b], Stefan Pischinger [a]

[a] Chair of Thermodynamics of Mobile Energy Conversion Systems, RWTH Aachen, Germany
[b] Institute of Thermodynamics and Sustainable Propulsion Systems, Technical University of Graz, Austria

HIGHLIGHTS

- Selective catalytic NO_X reduction for hydrogen-fueled internal combustion engines.
- Maximum NO_X conversion rate with Copper-SCR catalyst components.
- Negligible N_2O secondary emissions with Vanadium-SCR catalyst.
- Combination of the benefits from both catalyst types for zero-impact emissions.
- Complementary experiments on the model gas test bench and the engine test bench.

GRAPHICAL ABSTRACT



ARTICLE INFO

Keywords:
Exhaust gas aftertreatment
Hydrogen
Internal combustion engine
Nitrogen oxide
Pollutant emissions
Selective catalytic reduction

ABSTRACT

Hydrogen-fueled internal combustion engines are a promising CO_2-free and zero-impact emission alternative to battery or fuel cell electric powertrains. Advantages include long service life, robustness against fuel impurities and a strong infrastructural base with existing production lines and workshop stations. In order to make hydrogen engines harmless in terms of pollutant emissions as well, NO_X emissions at the tailpipe must be reduced as low as the zero-impact emission level. Here, the application of selective catalytic reduction (SCR) catalysts is a promising solution that can be rapidly adopted from conventional diesel engines.

This paper therefore investigates the influences of the hydrogen concentration in the raw exhaust gas, of the NO_2/NO_X ratio and of the space velocity on the performance of two different SCR technologies. The results show that both types of SCR, copper-zeolite and vanadium-based, have their advantages and drawbacks. Copper-based SCR catalysts have an early light-off temperature and reach maximum efficiencies of up to >99%. On the other hand, vanadium systems promise almost no secondary N_2O emissions. As a result, we combined both approaches to create a superior solution with high efficiency and lowest secondary emissions.

* Corresponding author.
E-mail address: stefan.sterlepper@rwth-aachen.de (S. Sterlepper).

https://doi.org/10.1016/j.apenergy.2023.122045
Received 28 July 2023; Received in revised form 19 September 2023; Accepted 27 September 2023
Available online 11 October 2023
0306-2619/© 2023 The Authors. Published by Elsevier Ltd. This is an open access article under the CC BY license (http://creativecommons.org/licenses/by/4.0/).

1. Introduction

The fight against climate change is one of the most pressing tasks of our time. For mobility applications, battery electric vehicles (BEVs) are considered as a sustainable solution, because they do not (locally) emit carbon dioxide (CO_2). Another option is to run internal combustion engines (ICE) on hydrogen, which also produces no CO_2 emissions. Apart from uncritical nitrogen, oxygen and water vapor, nitrogen oxides are the only major pollutant. [1,2] NO_X emissions are formed under high pressure and high temperature conditions in the combustion chamber. Changing the air/fuel ratio to lean conditions ($\lambda > 2$) is favorable for significantly reducing NO_X raw emissions by cooling the mixture and for decreasing fuel consumption by de-throttling.

Exhaust gas aftertreatment systems (EATS) are used to further reduce the NO_X raw emissions. To achieve zero-impact tailpipe emissions, where the concentration of pollutant does not affect air quality [3], several systems must be considered. For internal combustion engines in stoichiometric operation, three-way catalysts (TWC) are an option. However, at $\lambda = 1$ conditions, the high flame temperature leads to excessive NO_X raw emissions. Therefore, even with a very efficient TWC system, it is difficult to achieve zero-impact tailpipe emissions. In addition, stoichiometric operation has engine efficiency drawbacks [4].

During lean operation, NO_X storage catalysts (NSC) are an option. Intermittently operated NSCs store NO_X from the exhaust gas until a switch to the NO_X release or the regeneration mode is activated. The NO_X release can be achieved by increased temperature (passive NO_X adsorber, PNA) or the stored NO_X can be regenerated by a rich operation (lean NO_X trap, LNT). The passive control strategy for PNA applications requires close monitoring of the catalyst temperature but may not be able to achieve zero-impact emission levels as a single catalyst in all operating cases. On the other hand, the LNT must operate with hydrogen as the sole reducing agent (there is no significant concentration of hydrocarbon species as in established diesel applications). Here, high N_2O and/or NH_3 peaks can hardly be avoided when changing into regeneration mode [5,6,7].

In addition to NSCs, selective catalytic reduction (SCR) systems enable continuous lean operation. A urea-water solution (UWS) is dosed into the exhaust gas to produce ammonia as a reducing agent. Due to the urea carrier (CH_4N_2O), the dosing again adds carbon dioxide emissions to the exhaust. Therefore, raw NO_X emissions must be limited to limit urea consumption and stay below the 1 g_{CO2}/kWh limit that is expected to be the future definition of local carbon neutral operation [8,9]. For the ammonia-based SCR, the reaction mechanism in the Eqs. (1)–(6) compete. The so-called fast SCR reaction (Eq. (2)) builds on a NO_2 to NO_X ratio in the SCR inlet exhaust of $r_{NO_2/NO_X} = 50\%$. In case of a higher NO share, the slower Eq. (1) has to convert pure NO, whereas in higher NO_2 concentration, the UWS consumption increases (Eq. (3)). Since engine exhaust gases generally contain mainly NO, an oxidation catalyst is installed upstream of the SCR catalyst to form sufficient NO_2 amounts.

$$4\ NH_3 + 4\ NO + O_2 \rightarrow 4\ N_2 + 6\ H_2O \quad (1)$$

$$2\ NH_3 + NO + NO_2 \rightarrow 2\ N_2 + 3\ H_2O \quad (2)$$

$$8\ NH_3 + 6\ NO_2 \rightarrow 7\ N_2 + 12\ H_2O \quad (3)$$

$$4\ NH_3 + 3\ O_2 \rightarrow 2\ N_2 + 6\ H_2O \quad (4)$$

$$4\ NH_3 + 5\ O_2 \rightarrow 4\ NO + 6\ H_2O \quad (5)$$

$$4\ NH_3 + 4\ NO + 3\ O_2 \rightarrow 4\ N_2O + 6\ H_2O \quad (6)$$

N_2O is produced as an undesirable side reaction in SCR systems (Eq. (6)). N_2O has 300-times the global warming potential of CO_2 and this emission must be strongly limited or completely avoided [10]. A high selectivity towards N_2O production is a key property of suitable catalyst materials. From diesel applications, copper (Cu)-based zeolites are known to have early light-off, high NO_X reduction performance, but they also form N_2O emissions. As an alternative, Vanadium-based catalyst materials usually have a lower performance, but a higher N_2 selectivity. Last but not least, NH_3 slip over the SCR system needs to be avoided. In series applications, additional ammonia slip catalysts (ASC) convert remaining NH_3 emissions [11,12,13].

As an alternative to NH_3, H_2 can be used as the reducing agent in H_2-SCR systems. This is currently being investigated using platinum or palladium alloys as the catalytic material. The literature reports NO_X conversion rates up to and above $\eta_{NO_X} = 90\%$, but only in a small temperature window and with potentially high secondary N_2O emissions [14,15,16,17].

All catalyst systems need to reach their light-off temperature to start conversion. The time to light-off can be reduced by active catalyst heating measures. As with spark-ignition gasoline engines, late ignition timing can be an effective measure for H_2-ICEs to increase the exhaust gas temperature while accepting a deterioration in efficiency. Due to the wide ignition limits of hydrogen, stable operation is possible even at very late ignition angles. Other internal engine measures for catalyst heating can include increased idling or load point shifting. With a view to meeting EU7 emission standards, intensive investment is also being made in external heating measures. Here, heat is added to the exhaust gas by electrically heated discs ("eCat") or exhaust burners, using either electrical power or fuel combustion. Investigations in [18] have shown that external heaters can actually provide more heating power than internal heating measures. Beside eCat or exhaust burner, another possibility for external catalyst heating is to use the heat of hydrogen post-reactions in the exhaust gas system. That means that hydrogen is injected when the exhaust valve is open so that the unburnt fuel can be transferred to an oxidation catalyst in the exhaust system where it is oxidized to produce heat. Which catalyst heating strategy is the right one, is subject of much discussion and likely requires use-case specific assessments.

In summary, exhaust gas aftertreatment remains a significant challenge, even though H_2-ICEs produce only NO_X as major raw pollutant emission species. Compared to hydrogen-fueled ICEs, fuel cell electric vehicles (FCEVs) emit no pollutants. Especially at low loads, they are very efficient with system efficiencies of up to $\eta = 70\%$. Towards high load, the system efficiency drops down to $\eta = 50\%$ and thus into the potential efficiency range of H_2-ICEs. Meanwhile, the internal combustion engine has advantages in terms of robustness to fuel contamination or ambient conditions and the service life is transferable from diesel ICEs and so far much higher than for FCEVs. Existing production and maintenance infrastructure for ICEs enables quick market introduction and penetration. Hydrogen fuel stations and infrastructure can be used for both, H_2-ICEs and FCEVs.

As a result for the EATS, a fast development or identification of suitable systems is necessary to not hinder the quick market introduction potential of H_2-ICEs and to harvest the full climate gas reduction potential. At the same time, transfer from laboratory scale to series production still is time-consuming, whereas series production catalysts could be used immediately. Therefore, in this paper we aim to define the boundary conditions for a systematic catalyst screening procedure that enables efficient selection processes for individual H_2-ICE applications. As most established technology, we build on state-of-the-art SCR systems. The investigations are part of the project 1449 „Near-zero Emission Concept for H2 DI Otto Engines" funded by FVV e.V..

2. Experimental

2.1. Catalyst preparation

The experimental investigations were carried out on a model gas test bench (MGTB) and on an engine test bench as presented below. Both types of SCR catalysts were provided by Umicore AG & Co KG. The first is a state-of-the art copper-zeolite-based SCR catalyst with a cell density

of $\rho = 400\ cpsi$ and a wall thickness of $d = 4\ mil$. The type of the zeolite is Cu-SSZ-13. As an alternative with lower expected N_2O formation, a V_2O_5-WO_3-TiO_2 (VWT) coated SCR catalyst with the same cell density and wall thickness was selected.

Prior to the tests, the SCR catalysts were aged under conditions specified by the supplier. The Cu-based SCR samples were aged at $T = 700°C$ for $t = 10\ h$ with $\psi = 10\%$ water content in air, whereas the VWT-based samples were conditioned at $T = 600°C$ for $t = 50\ h$ with the same water content. Both aging conditions lead to comparable results, which was proven with a second Cu-SCR aged under the conditions applied for the VWT-SCR.

Furthermore, to complete the representative exhaust gas aftertreatment system at the engine test bench, Umicore AG & Co KG provided an oxidation catalyst (OC) with $\rho = 25\ g/ft^3$ platinum loading, an ammonia slip catalyst (ASC) with $\rho = 3\ g/ft^3$ platinum loading and a particulate filter (PF) coated with a $40/10\ g/ft^3$ palladium/ rhodium loading. The OC was aged at $T = 850°C$ for $t = 10\ h$ with $\psi = 10\%$ water content in air. The ASC was aged at $T = 700°C$ for $t = 10\ h$, while the PF was aged at $T = 700°C$ for $t = 10\ h$ both with $\psi = 10\%$ water content in air.

2.2. Setup of the model gas test bench

The investigations of the catalysts at synthetic, highly reproducible conditions were conducted at a Model Gas Test Bench of the Chair of Thermodynamics of Mobile Energy Conversion Systems (TME) of RWTH Aachen University. The schematic of the MGTB is shown in Fig. 1 and the overall capabilities and properties of the test bench can be found elsewhere [19,20,21,22,23].

For these investigations, the MGTB provides precise gas mixtures under various boundary conditions and is more flexible than an engine test bench due to its design. Thus, a broad screening of catalysts can be performed. To analyze a large spectrum of emissions up- and downstream of the catalyst, a Fourier-transform infrared spectrometer (FTIR) from MKS and a hydrogen mass spectrometer (HSense) were used in addition to the standard measurement devices such as FID, PMD and NDIR.

The catalyst sample is positioned downstream of the main heater and the gas mixer at the MGTB. The catalyst samples were drilled from the monolith, producing samples with a diameter of $d_{Cat} = 19.5\ mm$ and a length of $l_{Cat} = 108.2\ mm$.

During the tests, a temperature ramp from $T_{Start} = 180°C$ to $T_{End} = 500°C$ was run through with a temperature gradient of $\delta T/\delta t = 5\ K/min$. The concentrations of the gaseous components were derived from engine measurements. In principle, the level of the total NO_X emissions is set to $\psi_{NO_X} = 500\ ppm$ in $\psi_{O_2} = 10\%$ oxygen and $\psi_{H_2O} = 15\%$ water. Low concentrations of CO and CO_2 ($\psi_{CO} = 25\ ppm$ and $\psi_{CO_2} = 500\ ppm$) were added to simulate the emissions from unintended combustion of engine oil. For each measurement, the NH_3 to NO_X ratio was set to $\alpha = 1.5$ and the NO_2 to NO_X ratio was varied between $r_{NO_2/NO_X} = 0\%$ and $r_{NO_2/NO_X} = 75\%$.

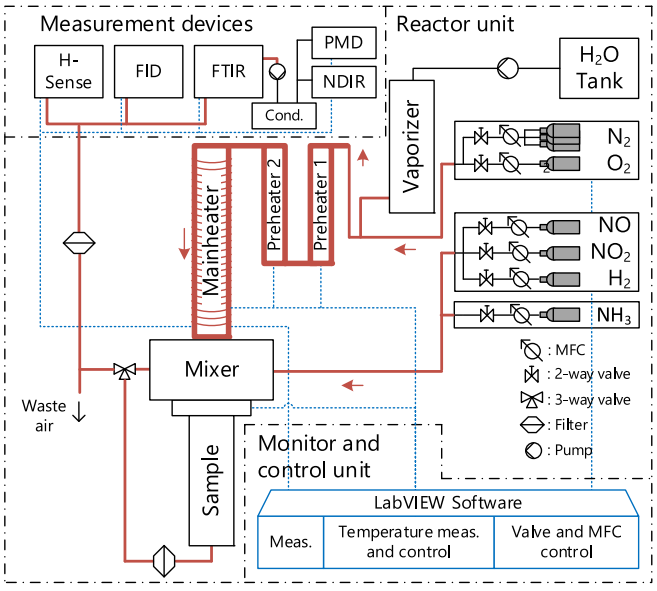


Fig. 1. Schematical Setup of the Model Gas Test Bench.

2.3. Setup of the multi-cylinder engine test bench

Experiments were conducted on the engine test bench at the Institute of Thermodynamics and Sustainable Propulsion Systems (ITNA) of the Technical University of Graz. The flexibility of the engine test bench in terms of exhaust gas composition or conditions is less than the model gas test bench but serves as a reference to ensure transferability into real-world applications. Therefore, a state-of-the-art in-line four-cylinder spark-ignited gasoline engine with two liters of displacement was adapted to run on hydrogen. Direct injection supplied gaseous hydrogen to the cylinders. The engine was operated under lean conditions with turbocharging, enabling most load points to run at a relative air-fuel ratio (lambda) of $\lambda > 2$.

Technical details of the engine are outlined in Table 1. Additional information concerning the engine can be found in [24]. The exhaust system is a prototype, designed with a modular approach to allow for easy replacements, such as the SCR catalyst. Fig. 2 illustrates a schematic representation of the engine and the exhaust system.

Up- and downstream of each catalyst, temperatures and pressures were measured. Various systems were utilized to analyze the exhaust gas, including a combustion emission bench, an FTIR spectrometer and a hydrogen mass spectrometer (HSense). A list of the analyzed emissions can be seen in Table 2. Each device could be used to analyze the exhaust gas via a gas line switched to different positions. Automotive lambda- and NO_X sensors were used to support the exhaust gas analyses. Data from the exhaust gas analyzers, engine parameters as well as information from sensors were centrally collected on the test bench computer. The information was then processed by computer software and either sent back to the engine or stored for further analysis.

Transient operation effects were investigated by the application of the "Worldwide Harmonized Light Vehicles Test Cycle" (WLTC). Based on the velocity profile, the power of the engine was calculated using PHEM, which is a simulation tool for longitudinal vehicle dynamics available from TU Graz. The simulation was conducted on a C-segment vehicle that weights $m = 1675\ kg$, has a seven gear automatic transmission and features start-stop functionality.

To obtain comparable results, the engine and exhaust aftertreatment system were conditioned in the same manner before each cycle. In order to approach real-world values for NO_X, N_2O and NH_3 emissions, the SCR catalyst was pre-conditioned regarding the NH_3 loading. Thereto, the SCR catalyst was emptied at $T_{SCR} = 300°C$ so that no NH_3 loading remained and subsequently loaded until one-third of its NH_3 storage capacity was reached. From that point onwards, the engine was switched off and both systems were cooled to a starting temperature of $T_{start} = 25°C$. The engine coolant was conditioned using a heat

Table 1
Technical specifications of the hydrogen engine.

Base Engine	Four-cylinder gasoline in-line (2.0 l TGDI)
Bore x Stroke	83 mm × 92 mm
Compression Ratio	9.8
Injection System	Hydrogen direct injection, central injector position
Ignition System	Modified series ignition coil; prototype spark plug
Boosting System	Series diesel turbocharger with VTG
Engine control	Prototype
Exhaust aftertreatment system	Prototype

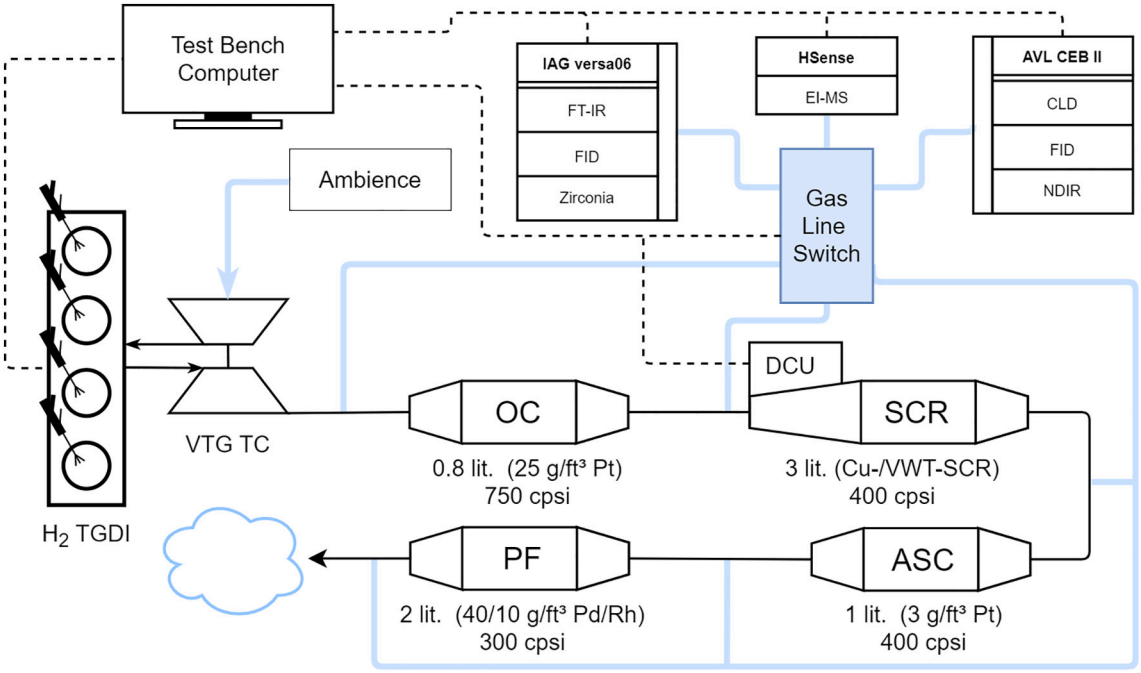


Fig. 2. Experimental setup of the multi-cylinder engine test bench.

Table 2
Measurement devices used for the exhaust gas analysis.

Measurement Device	Analyzer	Emissions
AVL CEB II	CLD	NO, NO_2
	NDIR	CO, CO_2
	FID	THC
IAG versa06	FTIR	NO, NO_2, N_2O, NH_3, …
	FID	THC
HSense	Mass Spectrometer	H_2

exchanger to reach the defined temperature. The coolant chills the engine and the lubricant oil. To additionally cool the system, fans blow air onto the oil pan and engine block to force convection. The exhaust aftertreatment system is cooled with a special method called RCD^+ (Rapid Cool-Down Plus) with which dry air flows through the exhaust system to avoid any water deposition on the SCR catalyst. Detailed descriptions of the RCD^+ method can be found in previous publications [25,26,37]. The cycles were performed at an ambient temperature of $T_{amb} = 23°C$ without any external heating or cooling of the coolant. Dosing of the urea-water solution (UWS) is enabled when the temperature upstream the SCR catalyst exceeds $T_{SCR} = 180°C$ to avoid any ammonium nitrate formation. The UWS is then dosed using a prototype dosing control unit, which aims at a temperature-dependent NH_3 loading state.

3. Results

3.1. Raw exhaust emissions of the hydrogen test engine

In this section, selected raw exhaust emissions of a two-liter hydrogen engine are presented. In a perfect hydrogen combustion, hydrogen and oxygen would solely react to form water [27]. Unfortunately, some side reactions occur during hydrogen combustion. Due to incomplete combustion of the air-fuel mixture, unburned H_2 can be detected in the exhaust gas. H_2 emissions are shown in the upper left diagram of Fig. 3. With premixed combustion, as is implemented in the hydrogen engine presented, the levels can increase to around 2000 ppm at lower part load. The downstream temperatures of the turbocharger are shown in the upper right diagram of Fig. 3. These temperatures may rise to about $T_{dsTC} = 500°C$ and drop to a minimum of roughly $T_{dsTC} = 250°C$ at idle, which suits catalysts better than comparable Diesel engines. According to Kühberger [26], comparable Diesel engines achieve more than $T_{dsTC} = 600°C$ in the full load, resulting in excessive temperatures in the exhaust gas catalysts.

NO_X emissions are generated in the combustion chamber when high temperatures are reached. Alastair [28] explains that NO_X emissions are formed due to the "Zeldovich mechanism" in all air-fuel mixture flames hotter than $T = 1300°C$. Klell et al. [27] report hydrogen combustion flame temperatures bigger than $T = 2000°C$, implying that the same NO_X formation mechanism also applies to hydrogen engines. As illustrated in the lower left diagram of Fig. 3, these emissions are minimal in the lower part load range, but can reach up to around $\psi_{NO_X} = 1000\ ppm$ at full load. These NO_X emissions contain NO and NO_2 species, along with others.

To provide an understanding of the NO_2 concentration in the exhaust gas of hydrogen engines, the NO_2 to NO_X ratio is shown in the lower right diagram of Fig. 3. The share of NO_2 in the NO_X emissions is generally low, with $r_{NO_2/NO_X} < 10\%$ across the entire engine map, excluding an anomaly at $n = 2000\ rpm$ and $BMEP = 16\ bar$ that cannot be explained yet. Multiple sources indicate that carbon-based emissions are negligible [29,18,30]. Since the study concentrates on the SCR performance, these species are not considered in this work.

3.2. Comparison of the Cu- and VWT-based SCR catalysts on a multi-cylinder hydrogen engine

In the tests of a multi-cylinder engine, a Cu-based and a VWT-based SCR catalyst were analyzed. Fig. 4 shows various measurement data, with the catalysts generally tested at temperatures from $T_{SCR} = 250°C$ to $T_{SCR} = 500°C$ at two different space velocities ($SV_{SCR} = 13500\ h^{-1}$ and $SV_{SCR} = 95000\ h^{-1}$). The catalysts were tested both with (w/) and without (w/o) an upstream oxidation catalyst to evaluate the influence of lower NO_2 to NO_X ratios and unburned hydrogen on the SCR technologies. The aim of the multi-cylinder engine experiments was to demonstrate how unburned hydrogen affects the different SCR technologies.

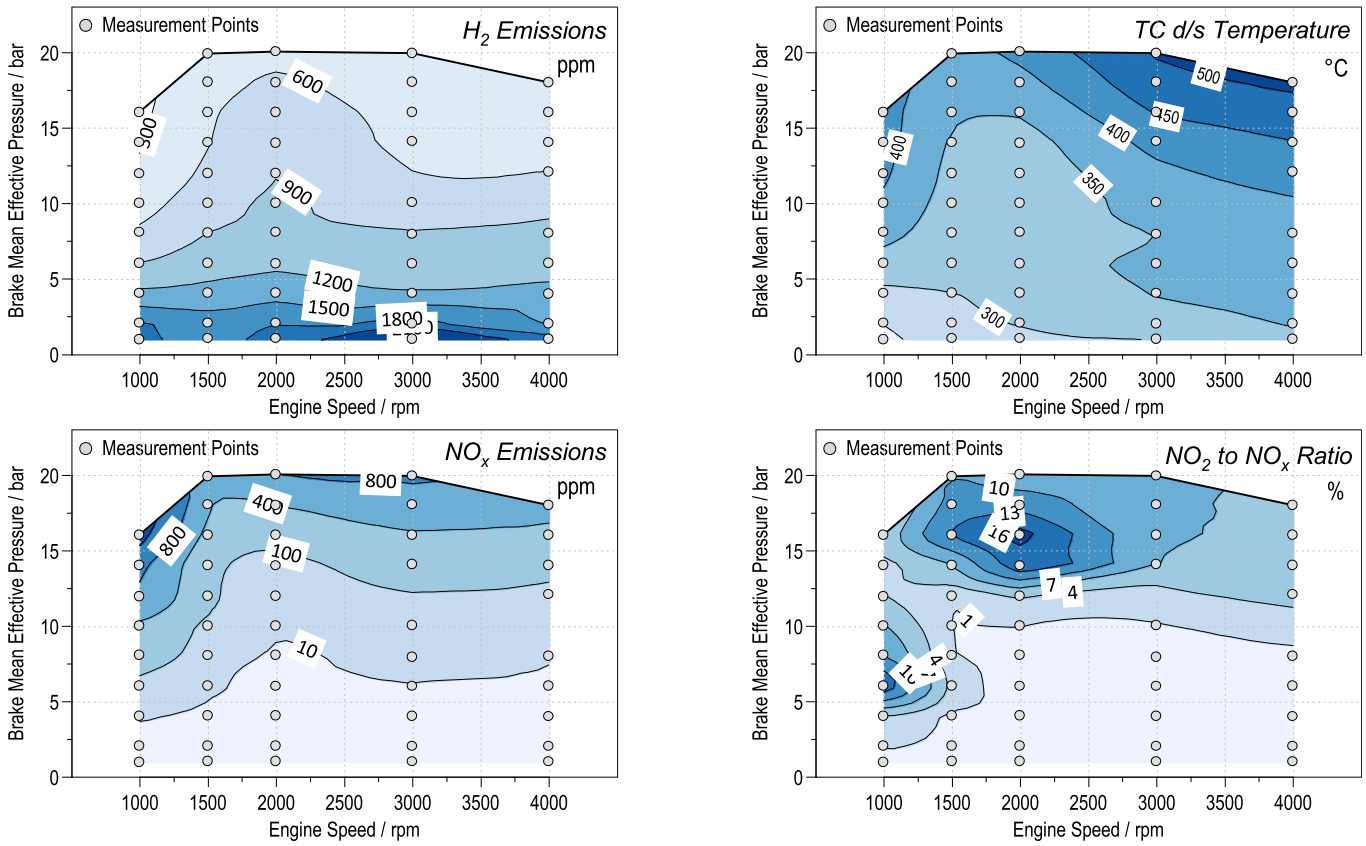


Fig. 3. Selected raw exhaust emissions of a two-liter hydrogen engine.

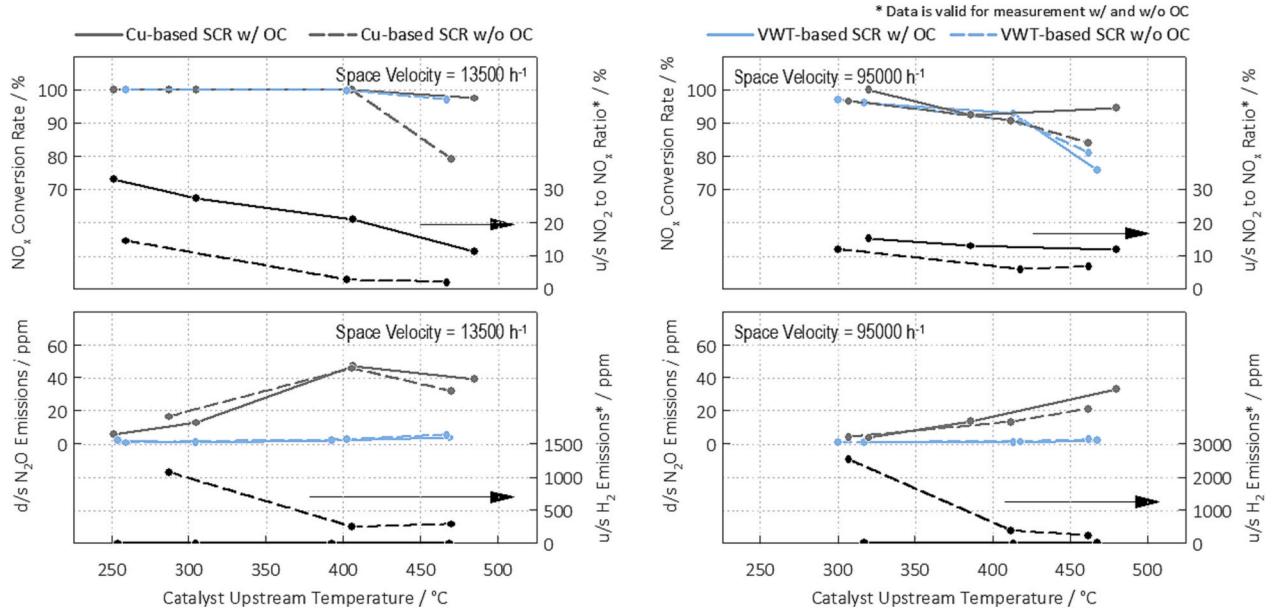


Fig. 4. Comparison of the performance of Cu-based and VWT-based SCR catalysts at two different space velocities with and without an upstream oxidation catalyst.

At the right ordinate of the upper diagrams of Fig. 4, the upstream NO_2 to NO_X ratio can be seen. This data is applicable to both SCR catalysts, since their upstream settings are the same. The dotted lines indicate the results without OC, whereas the solid lines represent the operation with an OC. It is evident that at both space velocities the NO_2 to NO_X ratio is increased by the OC, with the effect being smaller at the higher space velocity. The right ordinate of the lower diagram shows the upstream H_2 emissions. In the same manner as the NO_2 to NO_X ratio, this graph shows the upstream data as dotted lines. It can also be observed that at both space velocities, hydrogen is completely oxidized in the OC (full line, graphical overlay with x-axis).

At the left ordinate of the upper diagrams of Fig. 4, the NO_X conversion rates are shown. At the low space velocity (left diagram), all configurations except the Cu-based SCR catalyst without OC can

maintain almost full conversion at all exhaust temperatures analyzed. At the high space velocity (right diagram), increasing temperature results in reduced NO_X conversion performance. For the Cu-based SCR catalyst, the system with upstream OC reaches higher NO_X conversion rates, whereas there is no difference in NO_X conversion of the VWT-based SCR catalyst with or without OC. The implementation of an upstream oxidation catalyst yields higher NO_X conversion performance with the Cu-based SCR catalyst under high temperature or high space velocity conditions. One possible explanation for this is the shift towards a higher proportion of fast SCR reactions (Eq. (2)). However, the VWT-based SCR catalyst did not demonstrate a similar effect. For both catalysts, the influence of the presence or absence of hydrogen cannot be separated from the NO_2 to NO_X ratio effect. This issue will be addressed in the MGTB measurements discussed in Section 3.3.

At the left ordinate of the lower diagrams, the downstream N_2O emissions of the various configurations are shown. The Cu-based SCR catalyst emits higher N_2O quantities regardless of the space velocity. This observation aligns with literature results measured with diesel engines, e.g. by Yongjin et al. [31]. Observing the influence of hydrogen contents in the exhaust gas is not possible with this setup but will be investigated subsequently.

3.3. Comparison of the Cu-, VWT- and VWT-Cu-based SCR catalysts on the model gas test bench

For a comprehensive characterization of the catalysts, a series of experiments were performed on the MGTB to analyze the influence of the simulated exhaust gas of a hydrogen engine on the performance of the different types of SCR catalysts. In contrast to the internal combustion engine, the MGTB allows synthesis conditions where one parameter can be varied while all other parameters remain constant. Before investigating the influence of the hydrogen amount on the SCR reactions, the SCR performance of the Cu-based and VWT-based SCR catalysts were screened in a H_2-free atmosphere as found in the EATS setup with an OC (see Fig. 4). The NO_X conversion rate plotted versus the inlet catalyst temperature is shown in Fig. 5 for both catalysts.

The NO_2 to NO_X ratio at the inlet of the catalysts was varied between $r_{NO_2/NO_X} = 0\%$ and 75% for these measurements. In each figure, the NO_X conversion rate is plotted in the left diagram (Eq. (7)), whereas the N_2O concentration at the outlet of the catalyst can be seen in the lower right diagram. Another NO_X conversion rate considering also N_2O formation is added in the upper right diagram to point out the effect of the secondary emissions on the "real" NO_X conversion. This value is determined with Eq. (8), which considers 2 N-atoms in N_2O as not converted NO_X emission.

$$\eta_{NO_X} = \frac{\left(c_{NO,us} + c_{NO_2,us} - c_{NO_X,ds}\right)}{\left(c_{NO,us} + c_{NO_2,us}\right)} \tag{7}$$

$$\eta_{NO_X,N2O} = \frac{\left(c_{NO,us} + c_{NO_2,us} - c_{NO_X,ds} - 2c_{N_2O,ds}\right)}{\left(c_{NO,us} + c_{NO_2,us}\right)} \tag{8}$$

At an NO_2 to NO_X ratio of $r_{NO_2/NO_X} = 50\%$, both catalyst types show a comparable NO_X conversion performance over the complete temperature range. Once the NO_2 to NO_X ratio drops, the Cu-based SCR reaches a higher NO_X conversion rate η_{NO_X} at a lower temperature range between $T_{Start} = 180°C$ and $T_{Inlet} = 250°C$ and thus an earlier light-off. The NO_X conversion rate of the VWT-based SCR catalyst is apparently lower at NO_2 to NO_X ratio of $r_{NO_2/NO_X} = 0\%$, which is well known from literature [32]. A lower deNO_X performance can be observed at an NO_2 to NO_X ratio of $r_{NO_2/NO_X} = 75\%$ owing to the ammonium nitrate formation at low temperatures [33,34]. However, ammonium nitrate formation at the VWT-based SCR catalyst is more dominant at this NO_2 to NO_X ratio.

Another significant difference between both catalysts can be observed from their N_2O formation behavior. The Cu-based SCR catalyst produces a high amount of N_2O mainly via non-desired SCR reactions, as described in Section 1, particularly between the $T_{N_2O,start} = 200°C$ and $T_{N_2O,end} = 400°C$. The N_2O formation increases with the NO_2 level at the inlet of the catalyst. The VWT-based SCR catalyst forms less N_2O, leading to a higher corrected conversion rate and resulting in a better N_2 selectivity than the Cu-based SCR catalyst.

In the next step, the influence of H_2 on both SCR catalysts was investigated as seen in Fig. 6. These measurements were carried out to analyze the need of an oxidation catalyst upstream of the SCR catalyst for eliminating H_2 emissions. Looking at the Cu-based SCR results in Fig. 6 (a), no remarkable change of the NO_X conversion rate can be observed when varying the H_2 level at the inlet of the catalyst. A slightly higher N_2O formation can be seen in the lower right diagram, which is also reflected in the NO_X conversion rate considering N_2O emissions. However, the absolute increase of the N_2O concentration is in a range of $\Delta\psi_{N_2O} < 5\,ppm$, which is very low when comparing to the total amount

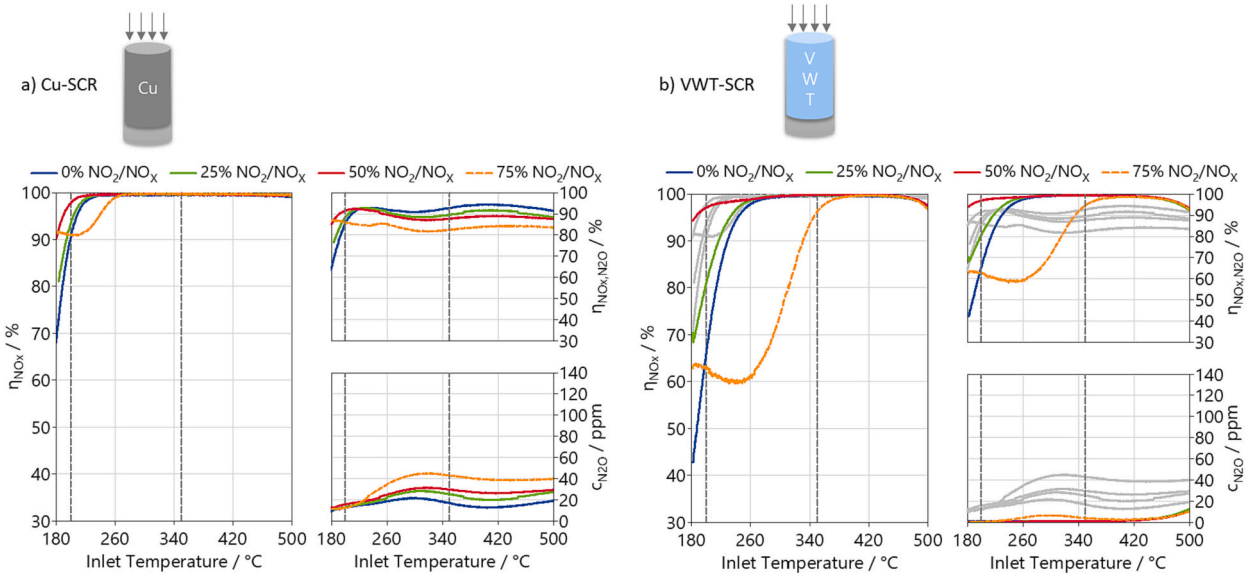


Fig. 5. Temperature dependent NO_X conversion rate (left), NO_X conversion rate considering N_2O emissions (upper right) and N_2O formation (lower right) for Cu-SCR (a) and VWT-SCR (b) catalysts at SV = 50,000 h^{-1}, $\psi_{NOx} = 500$ ppm, $\psi_{H2} = 0$ ppm, $\psi_{O2} = 10\%$, $\psi_{H2O} = 15\%$ from $T_{start} = 180°C$ to $T_{end} = 500\,°C$ at varying NO_2 to NO_X ratios between 0% and 75%; For reasons of comparison, in the background of (b) the graphs of (a) are repeated in light grey color.

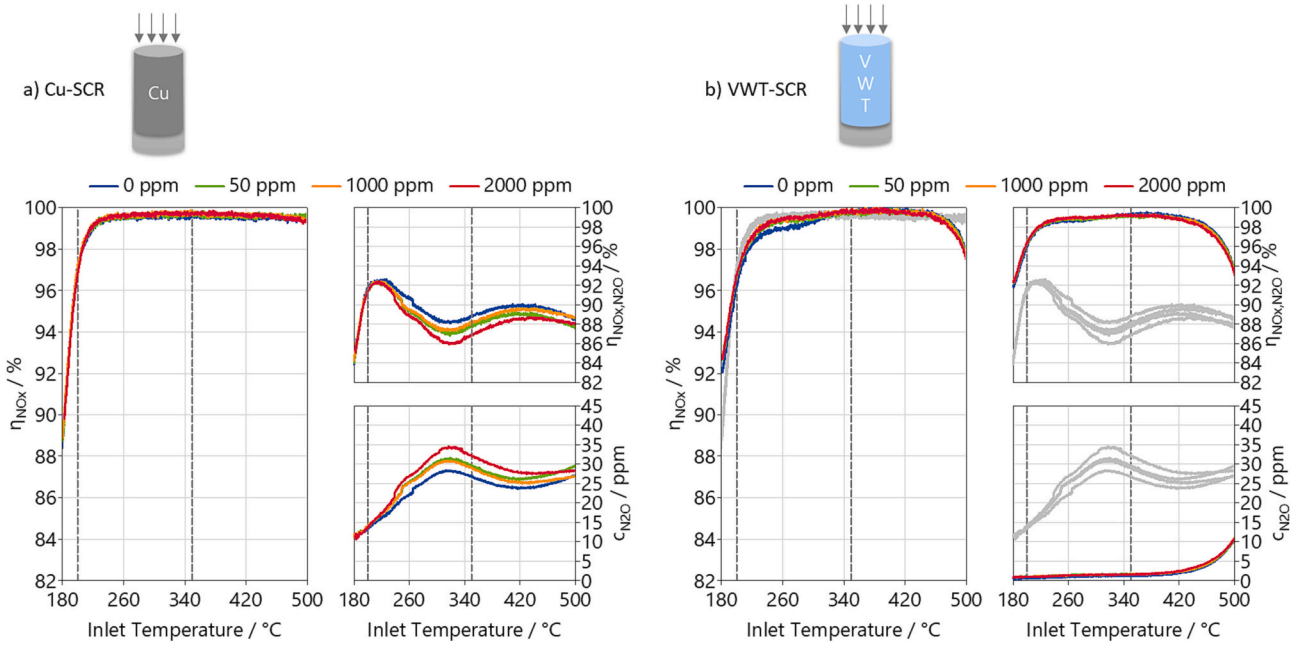


Fig. 6. Temperature and H_2 concentration dependent NO_X conversion rate (left), NO_X conversion rate considering N_2O emissions (upper right) and N_2O formation (lower right) for Cu-SCR (a) and VWT-SCR (b) catalysts at SV = 50,000 h^{-1}, ψ_{NOx} = 500 ppm, ψ_{H2} = 0 ppm, ψ_{O2} = 10%, ψ_{H2O} = 15% from T_{start} = 180°C to T_{end} = 500°C at an NO_2 to NO_X of 50% varying H_2 between ψ_{H2} = 0 and 2000 ppm; For reasons of comparison, in the background of (b) the graphs of (a) are repeated in light grey color.

of N_2O formation. On the right side of Fig. 6, it is obvious that hydrogen has no influence on the SCR reaction on the surface of VWT-based SCR catalyst.

To capture the influence of the hydrogen on the SCR catalyst, more challenging boundary conditions were tested on the MGTB. The space velocity was set to $SV_{SCR} = 150000\,h^{-1}$. These conditions represent medium to high engine load operation. As the oxidation catalyst is not able to form high amounts of NO_2 at this mass flow range, the NO_2 to NO_X ratio was decreased to $r_{NO_2/NO_X} = 25\%$ for these investigations to have a more realistic comparison. The results of these measurements are shown in Fig. 7 for both catalysts. Compared to the results shown in Fig. 6, the overall conversion rate is reduced for both catalysts. This is a result of reduced retention time on the catalyst surface. A minor additional reduction of the deNO_X performance with hydrogen present in the exhaust can be observed for the Cu-based SCR catalyst particularly at high temperatures of $T_{Inlet} > 400°C$. The NO_X conversion rate of the catalyst is reduced by up to $\Delta\eta_{NO_X} = 4\%$ with the increased H_2 level at the inlet. The difference between the curves for the H_2 concentration of

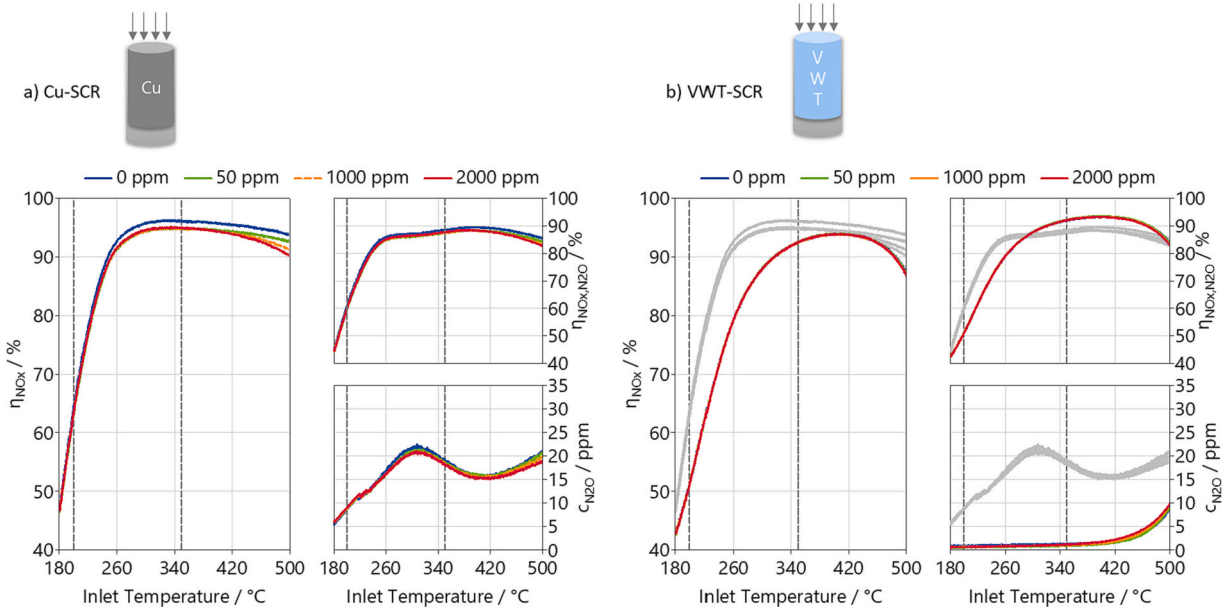


Fig. 7. Temperature and H_2 concentration dependent NO_X conversion rate (left), NO_X conversion rate considering N_2O emissions (upper right) and N_2O formation (lower right) for Cu-SCR (a) and VWT-SCR (b) catalysts at SV = 150,000 h^{-1}, ψ_{NOx} = 500 ppm, ψ_{H2} = 0 ppm, ψ_{O2} = 10%, ψ_{H2O} = 15% from T_{start} = 180°C to T_{end} = 500°C at an NO_2 to NO_X of 25% with varying H_2 between ψ_{H2} = 0 and 2000 ppm; For reasons of comparison, in the background of (b) the graphs of (a) are repeated in light grey color.

$\psi_{H_2} = 0\ ppm$ (blue line) and $\psi_{H_2} = 50\ ppm$ (green line) was presumably caused by a measurement inaccuracy. The offset between two curves is constant and for the full measurement, less than one percentage point of the total NO_X conversion rate, which is at the limit of detection. When considering the VWT-based catalyst, no influence of H_2 on the SCR reactions can be noted also under these boundary conditions.

The results show that both catalysts have advantages and disadvantages in reducing NO_X emissions from H_2 engines. The Cu-based SCR catalyst achieves early light-off temperatures for all relevant NO_2 to NO_X ratios, but on the other hand, it produces N_2O emissions, which are an additional pollutant and a greenhouse gas. In contrast, no N_2O emissions are produced in the VWT-based SCR catalyst. However, its NO_X conversion rate decreases as NO_2 to NO_X ratios decrease, which can be critical for some operating points. A combination of both technologies can compensate for these disadvantages.

To achieve this, the VWT-based SCR catalyst will be put in the first position to reduce the major amount of NO_X emissions without the drawback of N_2O formation. A Cu-based SCR catalyst in the second position can remove the remaining NO_X by utilizing its high efficiency at lower temperatures and different NO_2 to NO_X ratios. It can be expected that N_2O emissions will then be within reasonable limits since the absolute NO_X concentration at the inlet of the Cu-based SCR is already low. Both catalysts have the same length in the canning and half the size of the single catalysts.

To demonstrate the effects of this approach, a combined VWT-Cu SCR catalyst is prepared by installing both catalysts inline in one canning. The same measurement procedure was conducted as in Fig. 5 with a NO_2 to NO_X ratio of $r_{NO_2/NO_X} = 50\%$ as in the best case. The results of this measurement are compared with the corresponding results of the individual catalysts in Fig. 8. As can be seen in the left-hand diagram, the NO_X conversion performance is midway between the two individual catalysts. However, the secondary N_2O emissions of the combined version are much lower than for the Cu-based SCR. This difference is also reflected in the NO_X conversion rate considering the N_2O emissions in the upper right diagram.

This investigation shows that the concept of combining different types of catalysts can reduce the N_2O emissions while maintaining the NO_X conversion rate at acceptable levels. The ratio of the two SCR catalysts can be balanced between the desired NO_X conversion and acceptable N_2O formation for the target application.

Another important indicator for the performance and control of the SCR catalysts is the ammonia storage capacity. The Cu-based SCR catalyst showed the highest NH_3 storage capacity, while the VWT-based SCR catalyst could store 90% less. This can be explained by the zeolite structure of Cu-based SCR and can be applied under transient conditions when controlling the UWS dosage. A high ammonia storage capacity can decrease the UWS consumption and prevent the NH_3 slip during load steps, which is considered as a secondary emission.

3.4. Comparison of the transient behavior of the Cu- and VWT-Cu-based SCR catalysts

To assess the emission behavior during transient operation conditions, the combined VWT-Cu-based SCR catalyst was assessed against a pure Cu-based SCR brick using the "Worldwide Harmonized Light Vehicles Test Cycle" (WLTC). The vehicle speed profile and the engine power of the driving cycle are shown in the lower left diagram of Fig. 9. Starting at $T_{amb} = 27°C$, the temperature of the SCR catalyst can be seen at the left ordinate of the upper left diagram. As catalyst heating was not the focus of the project, no particular approach for catalyst heating has been employed. The release threshold for urea water solution dosing of $T_{SCR} = 180°C$ SCR catalyst upstream temperature leads to a start of dosing at $t = 520\ s$, once again without any dedicated heating strategy.

The left ordinate of the upper right diagram displays the NO_X conversion rates of the two catalysts, which were tested without any heat-up measures. In the first seconds, the conversion rate of both catalysts stays at $\eta_{NO_X} = 100\%$. This is due to the NO_X cold-storage ability of Cu-based SCR catalysts, which was also reported by Deinhofer et al. [35]. The pure Cu-based SCR catalyst maintains the cold-storage effect for a longer duration. After this phase, the stored NO_X emissions are withdrawn from the SCR catalysts. It can be observed that the Cu-based SCR catalyst also converts the withdrawn NO_X emissions (from $t = 50\ s$ to $t = 250\ s$) so that the conversion rate remains above $\eta_{NO_X} = 25\%$. The occurrence of NO_x conversion during a cold start by Cu-based SCR catalysts was also reported in [36].

Besides the NO_X conversion, a steep temperature increase in the middle of the Cu-based SCR catalyst can be seen in the upper left diagram (full grey line). This temperature increase is believed to be caused by water condensation, which was also reported in literature for Cu-zeolite-based SCR catalysts [36,18,35]. The VWT-Cu-based SCR catalyst on the other hand can only convert very little amounts of the withdrawn NO_X emissions in the first $= 250\ s$. Moreover, the increase in temperature is lower in the VWT-Cu SCR catalyst due to less water condensation in comparison to the Cu zeolite-based catalysts. For $t > 250\ s$, the VWT-Cu SCR catalyst outperforms the Cu zeolite-based catalysts in terms of NO_X conversion rate. This can be explained by a better temperature increase inside the VWT-Cu-based catalyst, as excessive water condensation occurs on a much lower basis. Towards the

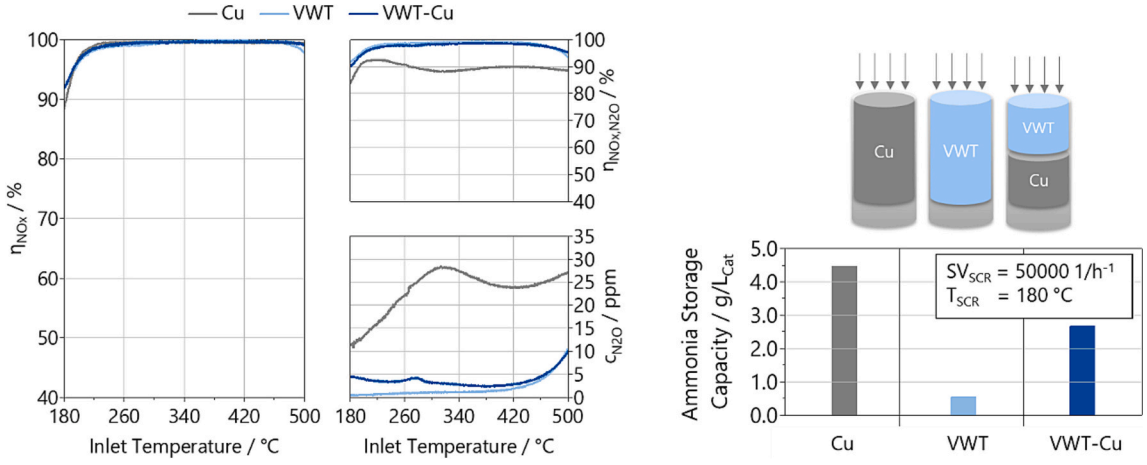


Fig. 8. Temperature dependent NO_X conversion rate (left), NO_X conversion rate considering N_2O emissions (upper right) and N_2O formation (lower right) and ammonia storage capacity for Cu-SCR, VWT-SCR and VWT-Cu-SCR catalysts at SV = 50,000 h^{-1}, $\psi_{NOx} = 500$ ppm, $\psi_{H2} = 0$ ppm, $\psi_{O2} = 10\%$, $\psi_{H2O} = 15\%$ from $T_{start} = 180°C$ to $T_{end} = 500\ °C$ at NO_2 to NO_X ratio of 50%.

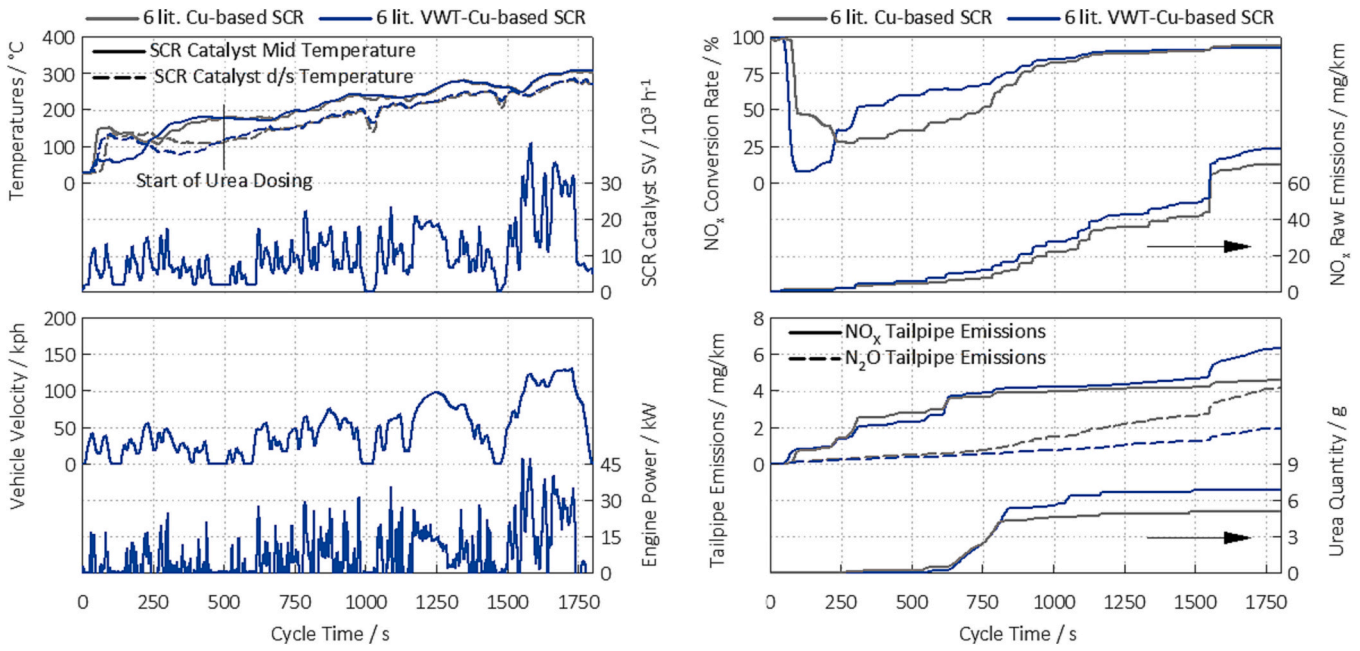


Fig. 9. Comparison of a Cu-based and a VWT-Cu-based SCR catalyst in a cold started WLTC with a H2-ICE with a displacement of $V_H = 2$ l and a vehicle mass of $m_{Veh} = 1680$ kg.

end of the driving cycle, when space velocities (displayed on the right ordinate in the upper left diagram) become high, the Cu-based SCR catalyst demonstrates its superior NO_X conversion performance.

In the total cumulative NO_X tailpipe emissions, which are shown on the left ordinate of the lower right diagram, the Cu-based SCR catalyst has a slight advantage over the combined VWT-Cu-based pendant. This advantage was expected since the NO_X conversion performance of the Cu-based SCR catalyst was observed at a higher level than the VWT-based one in Fig. 8 and before. Additionally, the dotted lines on the left ordinate of the lower right diagram show the N_2O emissions. Here, the VWT-Cu-based SCR catalyst shows significant potential in N_2O prevention. The lower right diagram illustrates the injected urea quantities. During the test run with the VWT-Cu-based SCR cycle, more urea was injected due to the higher NO_X raw emission level, which is shown on the right ordinate of the upper right diagram of Fig. 9. These differences in raw exhaust emissions emerge because the hydrogen engine is still at a very early prototype state. Nevertheless, the N_2O emissions stay lower with the VWT-Cu-based SCR catalyst, which emphasizes the N_2O prevention abilities of this type of catalyst. Table 3 provides a compact overview of the WLTP emission findings.

As can already be seen qualitatively in Fig. 8, Table 3 confirms that the combined VWT-Cu SCR catalyst successfully reduces N_2O emissions by over 50% compared to the Cu-based version. In terms of NO_X tailpipe emissions, the VWT-Cu-based SCR catalyst emits 6.33 mg/km. It should be noted that the NO_X raw emission level of this catalyst during testing was higher, measured at 78.67 mg/km compared to the corresponding Cu-based version, which showed levels of 73.23 mg/km. To account for these varying exhaust levels, the NO_X conversion rates can be compared. Here, the Cu-based SCR catalyst achieves an efficiency of $\eta_{Cu-SCR} = 93.75\%$, while the VWT-Cu-based one settles at $\eta_{VWT-Cu-SCR} = 91.35\%$.

Table 3
Exhaust emission results of the Cu- and VWT-Cu-based catalyst in the WLTC.

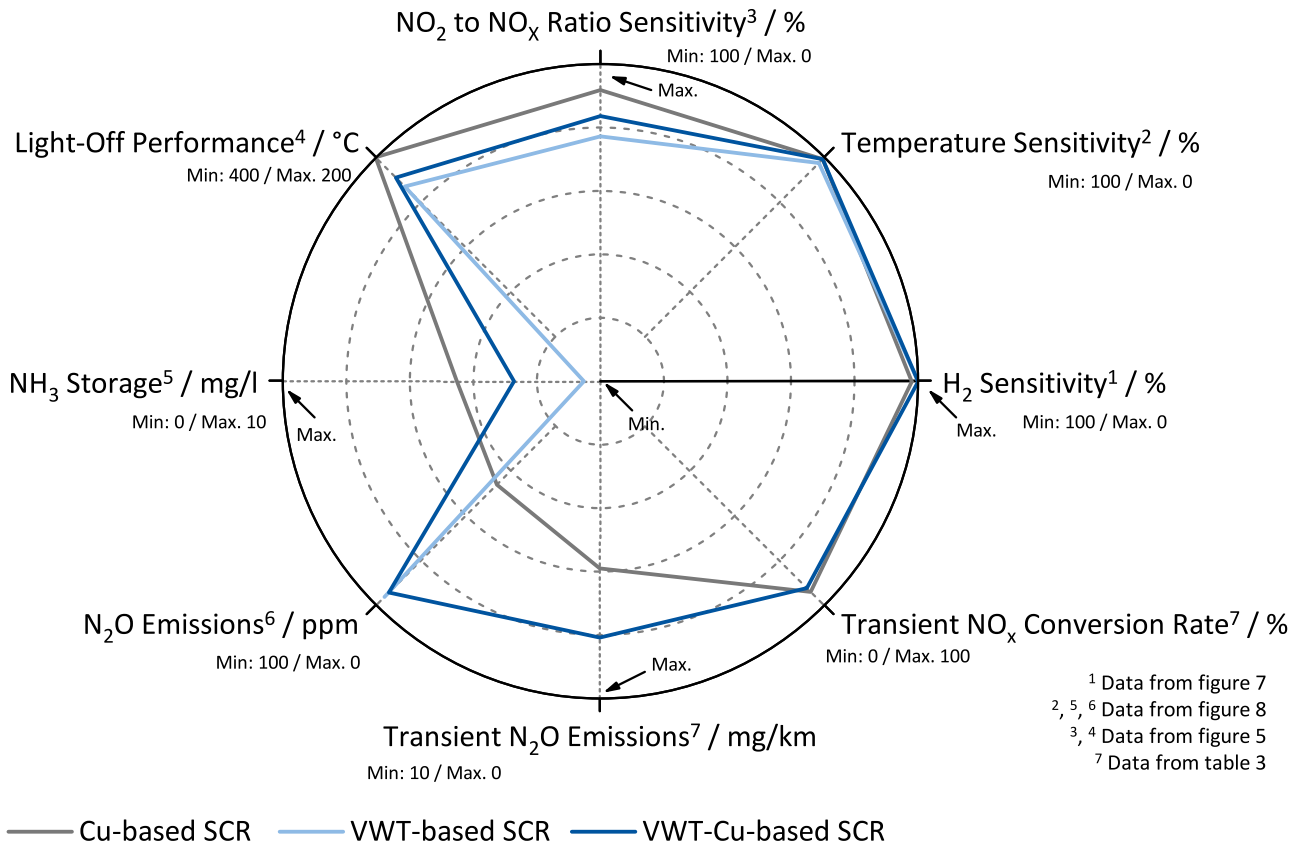
	Cu-based SCR catalyst	VWT-Cu-based SCR catalyst	
NO_X raw emissions	73.23	78.67	mg/km
NO_X TP emissions	4.57	6.33	mg/km
NO_X conversion rate	93.75	91.95	%
N_2O TP emissions	4.12	1.94	mg/km

4. Discussion

As explained in the introduction section, a short time to market is key for development of an exhaust gas aftertreatment system for hydrogen combustion engines. Therefore, two different state-of-the-art SCR catalyst types were investigated with the exhaust gas of an H_2-fueled internal combustion engine on both an engine test bench and a model gas test bench. From the results, a combination of both catalysts was derived as a third catalyst option. The parameters that have the greatest influence on the SCR system are summarized for all three types of catalysts in a net diagram in Fig. 10. Each axis of the diagram shows parameters, which were calculated based on data from either the MGTB or the engine test bench. The direction of the axes was chosen so that positive properties are on the outside. The origin of each data can also be found in the Fig. 10.

On the upper part of the diagram, the deNO_X performance parameters, including light-off performance, the sensitivity to the NO_2 to NO_X ratio, to the temperature as well as to the hydrogen, are presented. As a result, the Cu-based SCR catalyst exhibits superior light-off performance and a reduced sensitivity to the NO_2 to NO_X ratio. Furthermore, the Cu-based catalyst can provide greater ammonia storage capacity. The bottom section of the diagram provides details on secondary emissions. Here, the Cu-based SCR causes N_2O formation, whereas the VWT-based SCR and the combined VWT-Cu-based SCR emit almost none by taking advantage of the low N_2O formation tendency of the VWT-catalyst material. With that at hand, the advantages of the combined catalyst are evident.

So, what is the ideal configuration? From our point of view, the exhaust gas aftertreatment system must build on the knowledge gained with diesel engines to enable the advantageous rapid market introduction potential of hydrogen ICEs in the competition with fuel cell powertrains. Therefore, effective exhaust gas aftertreatment to minimize NO_X emissions from hydrogen-fueled internal combustion engines should include an oxidation catalyst and an SCR catalyst with aqueous



[1] Reduction in NO_X conversion rate at 350 °C, 150k 1/h, 50% NO_2/NO_x, Var. H_2
[2] NO_X conversion rate at 500 °C, 50k 1/h, 50% NO_2/NO_x, No H_2
[3] Reduction in NO_X conversion rate from 50 to 0% NO_2/NO_x at 200 °C, 50k 1/h, No H_2
[4] Temperature for 95% NO_X conversion rate at 50k 1/h, 25% NO_2/NO_x, No H_2
[5] NH_3 Starage Capacity at 300 °C, 50k 1/h, 50% NO_2/NO_x, No H_2
[6] N_2O Emissions at 340 °C, 50k 1/h, 50% NO_2/NO_x, No H_2
[7] Data from the WLTC driving cycle (Data for VWT-based catalyst was not available)

[1] Normalized Value ($\eta_{NOx,2000\ ppm\ H2}/\eta_{NOx,\ 0\ ppm\ H2}$ @ 350 °C)
[2] Actual Value
[3] Normalized Value ($\eta_{NOx,0\ \%\ NO2/NOx}/\eta_{NOx,50\ \%\ NO2/NOx}$ @ 200 °C)
[4] Actual Value
[5] Actual Value
[6] Actual Value
[7] Actual Value

Fig. 10. Normalized influence parameters of the investigated SCR catalysts.

urea solution dosing. However, Fig. 10 demonstrates that the catalyst system for lean-burn hydrogen combustion engines is a compromise between NO_X conversion performance and secondary emission formation. Thus, the selection of the system must be based on consideration of the boundary conditions.

The comparison of representative Cu- and VWT-based SCR catalysts led to the conclusion that a combination of both could be beneficial. As a result, we suggest a combined SCR system with a VWT-based catalyst in front to convert NO_X emissions with minimal N_2O formation and a Cu-based catalyst at the rear position to effectively reduce any remaining NO_X emissions. Due to the low amount of NO_X reaching the second SCR brick, the N_2O formation of the Cu-based SCR catalyst is also very low. In this investigation, the selected catalysts were of similar size, but a higher proportion of the VWT-based SCR catalyst or an overall larger catalyst volume may lead to further improvements. A larger catalyst volume would decrease space velocities, which has been shown to be an important factor in catalyst efficiency in these studies, but it presents challenges in terms of cost and packaging requirements.

As anticipated from encounters with other lean-combustion engines, the variation of the NO_2 to NO_X ratio shows that the earliest light-off performance can be achieved at a NO_2 to NO_X ratio of $r_{NO_2/NO_X} = 50\%$. This applies for both SCR types investigated as well as for their combination and highlights the benefits of implementing an oxidation catalyst upstream of the SCR catalyst to sustain optimal NO_2 to NO_X ratios that ensure high conversion rates at lower catalyst temperatures. Alternatively, cold start measures can be used to reduce the warm-up time to the light-off point with overall high conversion rates at all NO_2 to NO_X ratios. To limit secondary emissions such as ammonia or particulate emissions, an ASC-coated particulate filter can also be used in the fourth position, but this was not within the scope of this study.

The investigations on the engine test bench were carried out using a modified ICE that was not fully optimized for hydrogen use. In the future, dedicated H_2-ICEs are anticipated to feature improved mixture formation, leading to a decrease in H_2 raw emissions. Nonetheless, the exhaust gas aftertreatment system is not expected to be greatly impacted by the reduced hydrogen fraction. For both materials, it was generally found that hydrogen emissions in the exhaust gas have a minimal impact on the functionality of the SCR.

5. Conclusions

In this work, experimental investigations on the emissions were conducted to determine the zero-impact emission potential of hydrogen engines. An initial characterization of the two-liter hydrogen engine resulted in a hydrogen raw emission range of $300\,ppm \leq \psi_{H_2} \leq 2000\,ppm$ and an exhaust temperature range of $250°C \leq T_{ds,TC} \leq 550°C$ at stationary operation. Nitrogen oxides (NO_X) raw emissions were measured with $\psi_{NO_x} \leq 100\,ppm$ (mostly NO) for a large area of the engine map, increasing only at higher loads and especially at low-end torque.

In order to reduce the NO_X emissions, two selective catalytic reduction (SCR) catalysts, namely Copper-zeolite and VWT (V_2O_5-WO_3-TiO_2), were investigated. Both materials origin from series production systems to allow for a rapid introduction of the hydrogen internal combustion engine (H_2-ICE) upon successful implementation. Stationary investigations at the engine test bench result in good SCR performance for both systems at low space velocity and moderate temperatures. With increasing space velocity and temperature an efficiency decline is observed, potentially caused by hydrogen emissions in the exhaust or by a low NO_2/NO_X ratio. To differentiate between the parameters, detailed variations followed on the model gas test bench. From the engine and model gas investigations, the following findings apply:

- Hydrogen engines emit NO and NO_2 emissions especially at full-load and under transient engine operation, which must be reduced by exhaust gas aftertreatment to achieve zero-impact emission levels.
- A carry-over of a diesel exhaust gas aftertreatment systems can enable lowest tailpipe emissions for H_2-ICEs down to zero-impact emissions at stationary low to medium load operation. For high load and transient conditions, hydrogen engine-specific characteristics need further investigations.
- Similar to diesel applications, SCR catalysts enable a very efficient NO_X removal with highest efficiency at $r_{NO_2/NO_X} = 50\%$, where the so-called fast SCR reaction dominates. In this work, the Cu-based SCR is capable of higher overall NO_X conversion rates η_{NO_X} than the chosen VWT-based SCR.
- The VWT-based SCR shows more sensitivity to a variation of the NO_2/NO_X ratio than the Cu-based SCR. Low NO_2/NO_X ratios lead to delayed light-off points for both catalysts, but much more significantly for the VWT-based SCR type. At a high NO_2/NO_X ratio of $r_{NO_2/NO_X} = 75\%$, a strong decrease of the NO_X conversion performance of the VWT-based SCR down to $\eta_{NO_X} = 60\%$ is attributed to ammonium nitrate formation.
- The Cu-based SCR results in N_2O emission formation up to $c_{N_2O} > 40\,ppm$, whereas no significant nitrous oxide formation is detected with the VWT-based SCR. Upon subtracting secondary N_2O emissions, the corrected NO_X conversion $\eta_{NO_X,N2O}$ is higher for the VWT-based SCR, indicating a more effective reduction of NO_X to N_2.
- Adding up to $\psi_{H_2} = 2000\,ppm$ hydrogen to the exhaust gas shows no significant effect on the NO_X conversion performance of both catalysts. Only for the Cu-based SCR a minor increase of secondary N_2O emissions is measured.
- As the space velocity increases (here to $SV = 150000\,h^{-1}$) the catalytic effect of both catalysts decreases, both in terms of NO_X reduction and N_2O formation. At these challenging conditions, the difference in light-off performance becomes apparent, with the Cu-based SCR superior to the VWT-based SCR.

Based on the findings above, the Copper-based SCR catalyst has advantages in total NO_X conversion rates and light-off performance and is less sensitive to variations of the NO_2/NO_X ratio. The VWT-based SCR however, leads to very low N_2O formation, resulting in a higher NO_X reduction rate to nitrogen at most conditions. To conclude, the implications are as follows:

- An optimal NO_2/NO_X ratio of $r_{NO_2/NO_X} = 50\%$ requires an effective (and potentially expensive) oxidation catalyst upstream of the SCR systems. However, this ratio is only required for high cold start performance. Thus, the oxidation catalyst could also be replaced by or combined with other cold start measures, e.g. the integration of an electrically heated disc.
- Hydrogen emissions in the exhaust have no significant effect on the SCR performance. Further investigations are necessary to quantify oxidation effects of hydrogen in an exhaust gas aftertreatment without any specific oxidation catalyst, in order to estimate climate gas effects of potential hydrogen tailpipe emissions.
- A combination of two SCR catalysts, with the VWT-based brick in first and the Cu-based one in second position enables the utilization of the advantages of both. In an optimal system, the VWT-based SCR catalyst reduces the major part of the NO_X emissions without any N_2O formation. The subsequent Cu-based SCR catalyst needs to convert only small amounts of NO_X and therefore causes only minor secondary N_2O emissions. In this work, an equal volume split between the two catalysts already shows positive effects. For series applications, a higher volume fraction of the VWT-based SCR catalyst could be beneficial, if the cold start performance allows.
- In the transient driving cycle (WLTC), the use of a VWT-based SCR catalyst in the first position, followed by a Cu-based catalyst in the second position, effectively reduces N_2O emissions while maintaining a similar NO_X conversion rate. Furthermore, the combination of the VWT-Cu-based catalyst results in reduced water condensation, preventing temperature drops in the catalyst that are common with pure Cu-based SCR catalysts.

In summary, a combination of a small (low PGM) oxidation catalyst in the first position, a VWT-based SCR catalyst in the second position, and a Cu-based SCR catalyst in the third position takes advantage of all three components without increasing the costs of the exhaust gas aftertreatment system. Investigations on the emissions from hydrogen engines can be followed with analyses of the catalyst aging behavior under hydrogen engine exhaust gas conditions, as the potential aging effect of a high water content has not yet been clarified.

Funding

This research was funded by FVV e.V., project number 1449.

CRediT authorship contribution statement

Can Özyalcin: Writing – original draft, Investigation, Conceptualization. **Stefan Sterlepper:** Writing – review & editing, Conceptualization. **Sebastian Roiser:** Writing – original draft, Investigation, Conceptualization. **Helmut Eichlseder:** Writing – review & editing, Supervision. **Stefan Pischinger:** Writing – review & editing, Supervision.

Declaration of Competing Interest

The authors declare that they have no known competing financial interests or personal relationships that could have appeared to influence the work reported in this paper.

Data availability

Data will be made available on request.

Acknowledgements

The authors would like to thank Claus Wundling and David Lejsek (both Robert Bosch GmbH) for the chairmanship and the FVV working group for their valuable discussions, ideas and support in carrying out the corresponding research project. Many thanks also go to Umicore AG & Co. KG for providing the catalyst components.

References

[1] Verhelst S, Wallner T. Hydrogen-fueled internal combustion engines. Prog Energ Combust Sci, Elsevier 2009;35:490–527. https://doi.org/10.1016/j.pecs.2009.08.001.

[2] Verhelst S. Recent progress in the use of hydrogen as a fuel for internal combustion engines. Int J Hydrogen Energy 2013. https://doi.org/10.1016/j.ijhydene.2013.10.102. Elsevier.

[3] Maurer R, Kossioris T, Hausberger S, Toenges-Schuller N, Sterlepper S, Günther M, et al. How to define and achieve zero-impact emissions in road transport? Transp Res Part D Transp Environ 2023. https://doi.org/10.1016/j.trd.2023.103619.

[4] Fischer M, Sterlepper S, Pischinger S, Seibel J, Kramer U, Lorenz T. Operation principles for hydrogen spark ignited direct injection engines for passenger car applications. Int J Hydrogen Energ 2022. https://doi.org/10.1016/j.ijhydene.2021.11.134.

[5] Abdulhamid H, Fridell E, Skoglundh M. Influence of the type of reducing agent (H2,CO,C3H6and C3H8)on the reduction of stored NOXin a Pt/BaO/Al2O3model catalyst. Top Catal 2004. https://doi.org/10.1023/B:TOCA.0000029745.87107.b8. Plenum Publishing Corporation.

[6] Lindholm A, Currier NW, Fridell E, Yezerets A, Olsson L. NOx storage and reduction over Pt based catalysts with hydrogen as the reducing agent: influence of H2O and CO2. Appl Catal Environ 2007. https://doi.org/10.1016/j.apcatb.2007.03.008. Elsevier.

[7] Schönebaum S, Dornseiffer J, Mauermann P, Wolkenar B, Sterlepper S, Wessel E, et al. Composition/performance evaluation of lean NOx trap catalysts for coupling with SCR technology. ChemCatChem Chem Eur 2021. https://doi.org/10.1002/cctc.202001761.

[8] European Commission Regulation (EU) 2019/1242 of the European Parliament and of the Council of 20 June 2019 setting CO2 emission performance standards for new heavy-duty vehicles. Off J Eur Union. 2019. https://eur-lex.europa.eu/eli/reg/2019/1242/oj. OJ L 198, 25.7.2019, p. 202–240.

[9] Hydrogen Europe. Hydrogen europe position paper - CO2 emission standards for heavy-duty vehicles. 2023.

[10] Pachauri RK. Climate change 2007: Synthesis report: A report of the Intergovernmental Panel on Climate Change. Geneva: IPCC, WMO; 2008.

[11] Jansson J. Vanadia-based catalysts for mobile SCR. In: Nova I, Tronconi E, editors. Urea-SCR technology for deNOx after treatment of diesel exhausts. New York: Springer New York; 2014. p. 65–96.

[12] Johnson TV. Review of selective catalytic reduction (SCR) and related technologies for mobile applications. In: Nova I, Tronconi E, editors. Urea-SCR technology for deNOx after treatment of diesel exhausts. New York: Springer New York; 2014. p. 3–31.

[13] Schmieg SJ, Lee J-H. Evaluation of supplier catalyst formulations for the selective catalytic reduction of NOx with ammonia. In: SAE technical paper series; 2005. pp. SAE 2005-01-3881.

[14] Savva PG, Costa CN. Hydrogen lean-DeNOx as an alternative to the ammonia and hydrocarbon selective catalytic reduction (SCR). Catal Rev Sci Eng 2011. https://doi.org/10.1080/01614940.2011.557964.

[15] Schott FJP, Balle P, Adler J, Kureti S. Reduction of NOx by H2 on Pt/WO3/ZrO2 catalysts in oxygen-rich exhaust. Appl Catal Environ 2009;87(1–2).

[16] Leicht M, Schott FJP, Bruns M, Kureti S. NOx reduction by H2 on WOx/ZrO2-supported Pd catalysts under lean conditions. Appl Catal Environ 2012. https://doi.org/10.1016/j.apcatb.2012.01.023. Elsevier.

[17] Hamada H, Haneda M. A review of selective catalytic reduction of nitrogen oxides with hydrogen and carbon monoxide. Appl Catal A Gen 2012;421–422:1–13.

[18] Roiser S, Beringer S, Schutting E, Eichlseder H, Rabe T, Krinn I, et al. Driving hydrogen engines towards a zero-impact emission level. In: 10. international engine congress 2023, Baden-Baden; 2023.

[19] Wolkenar B, Schönebaum S, Mauermann P, Dittmann P, Pischinger S, Simon U. Storage and oxidation of oxygen-free and oxygenated hydrocarbons on a Pt–Pd series production oxidation catalyst. Top Catal 2019;62:376–85.

[20] Özyalcin C, Mauermann P, Dirkes S, Thiele P, Sterlepper S, Pischinger S. Investigation of filtration phenomena of air pollutants on cathode air filters for PEM fuel cells. Catalysts 2021;11(11):1339.

[21] Schönberger AA, Haselmann GM, Wolkenar B, Schönebaum S, Mauermann P, Sterlepper S, et al. Sorption and reaction of biomass derived HC blends and their constituents on a commercial Pt–Pd/Al2O3 oxidation catalyst. Catal Lett 2022;152(6):1880–94.

[22] Özyalcin C, Mauermann P, Dornseiffer J, Sterlepper S, Günther M, Pischinger S. Contributions of washcoat components in different configurations to the NOx and oxygen storage performance of LNT catalysts. Catalysts 2022;12(9):953.

[23] Schönberger Alvarez AA, Özyalcin C, Padeken T, Mauermann P, Lehrheuer B, Sterlepper S, et al. Impact of unintentionally formed CH2O in oxygenated fuel exhausts on DeNOx-SCR at different NO2/NOx ratios under close to real conditions. Cat Sci Technol 2023;13:4069–81. https://doi.org/10.1039/D2CY01935C.

[24] Seboldt D, Mansbart M, Und GP. Wasserstoffmotoren für zukünftige Pkw und leichte Nutzfahrzeuge. MTZ; 02 2021. p. 46–51.

[25] H. Wancura, G. Kühberger and B. Gamper, Verfahren zur beschleunigten Konditionierung eines Verbrennungsmotorsystems vor Durchführung eines Kaltstartemissionstests. Austria Patent 50650/2021, 2021.

[26] Kühberger G. Ultrafast catalyst light-off strategy for extended NOx emission control of CI-engines for 48V based hybrid electric vehicles. Graz: Graz University of Technology; 2022.

[27] Klell M, Eichlseder H, A T. Wasserstoff in der Fahrzeugtechnik. Wiesbaden: Springer Fachmedien Wiesbaden; 2018.

[28] Alastair L. Optimising air quality co-benefits in a hydrogen economy: a case for hydrogen-specific standards for NOx emissions. Environ Sci Atmos 2021:201–7. Heslington, Royal Society of Chemistry.

[29] Schutting E, Roiser S, Eichlseder H, Lux S, Kleiber S. Hydrogen engine exhaust aftertreatment. In: 43. Internationales Wiener Motorensymposium, Vienna; 2022.

[30] Roiser S, Christoforetti P, Schutting E, Eichlseder H. Emission behaviour and aftertreatment of stationary and transient operated hydrogen engines. SAGE J 2023;0(0). https://doi.org/10.1177/14680874231172316.

[31] Yongjin J, Young JS, Young DP, Chong PC, Jinyoung J, Gangchul K. NOx and N2O emissions over a urea-SCR system containing both V2O5-WO3/TiO2 and Cu-zeolite catalysts in a diesel engine. Chem Eng J 2017;326:853–62.

[32] Ciardelli C, Nova I, Tronconi E, Chatterjee D, Bandl-Konrad B. A "nitrate route" for the low temperature "fast SCR" reaction over a V2O5-WO3/TiO2 commercial catalyst. Chem Commun (Camb) 2004:2718–9.

[33] Koebel M, Madia G, Elsener M. Selective catalytic reduction of NO and NO2 at low temperatures. Catal Today 2002;73:239–47.

[34] Madia G, Koebel M, Elsener M, Wokaun A. Side reactions in the selective catalytic reduction of NOx with various NO2 fractions. Ind Eng Chem Res 2002;41(16):4008–15.

[35] Deinhofer L, Maurer M, Barnstedt G, Keber A. Analysis of the NOx storage behaviour during cold start of modern SCR flow-through substrates and SCR onfilter substrates. Automotive Engine Technol 2022;7:81–96. Springer Nature.

[36] Deinhofer L, Maurer M, Barnstedt G, Keber A. Modelling of the NOx storage behaviour during cold start of modern zeolite SCR catalysts. Automotive Engine Technol 2022:353–68. Springer Nature.

[37] Schutting E. Method for accelerated EAS cold start cycle measurements. Vienna: Austrian Research Promotion Agency; 2021.